Journal of Alloys and Compounds 498 (2010) 113–117

Contents lists available at ScienceDirect

Journal of Alloys and Compounds

journal homepage: www.elsevier.com/locate/jallcom

Effect of grain size on magnetic and nanomechanical properties of $Co_{60}Fe_{20}B_{20}$ thin films

Yuan-Tsung Chen*, C.C. Chang

Department of Materials Science and Engineering, I-Shou University, Kaohsiung 840 Taiwan, ROC

ARTICLE INFO

Article history:
Received 23 February 2010
Received in revised form 16 March 2010
Accepted 17 March 2010
Available online 24 March 2010

PACS:
62.25+g
75. 60. Nt
75. 70.−i
68.37.Lp
74.25.Ha

Keywords:
Magnetic tunneling junctions (MTJs)
Annealing
Nano-indentation
Grain size effect

ABSTRACT

In this investigation, CoFeB thin films were sputtered onto glass substrates with thicknesses (t_f) from 100 to 500 Å under the following conditions; (a) substrate temperature (T_s) maintained at room temperature (RT), (b) post-annealing at heat annealing T_A = 150 °C for 1 h, and (c) post-annealing at heat annealing T_A = 350 °C for 1 h. X-ray diffraction (XRD) reveals that CoFeB films are nano-crystalline at RT, and become more crystalline with post-annealing treatment. To determine the grain size distribution, the plane-view microstructure was observed under a high-resolution transmission electron microscope (HRTEM). The selected-area-diffraction (SAD) patterns obtained using HRTEM support the XRD results. The X-ray diffraction peak and the electron diffraction pattern demonstrate that the CoFeB thin film had a nano-crystallization body-centered cubic (BCC) CoFeB (1 1 0) at RT. Following annealing treatment, the CoFeB BCC (1 1 0) structure was more crystalline. Increasing the post-annealing temperature from RT increases the grain size. Additionally, the grain size distributions under various conditions are determined using plane-view HRTEM. The magnetic remanence properties of the CoFeB thin films are sensitive to grain size. This result shows that grain size refinement reduces effective anisotropy, increasing the ferromagnetic exchange coupling, and thereby remanence. The coercivity (H_c) is also observed to increase, since the grain size distribution is enlarged. Based on the relationship between grain size and the nano-indentation results, the decline in the hardness and Young's modulus can be reasonably inferred to be associated with an enlarged grain size, consistent with the "Hall–Petch" effect and the grain refinement mechanism.

1. Introduction

Recently, magnetic tunnel junctions (MTJs) have been of particular interest for use in magnetoresistance random access memory (MRAM), read head, and gauge sensor applications [1–6]. Magnetic CoFeB, Co, or NiFe thin film can be inserted as a free and/or pinned layer into the MTJ device, as it has a high spin tunneling efficiency and its spin-valve structure exhibits ferromagnetism (FM)/antiferromagnetism (AFM) exchange-biasing anisotropy [7–10]. Moreover, the favorable characteristics of the MTJ device, including high tunneling magnetoresistance (TMR), strength, and durability, are critical to operation of an MTJ device at room temperature (RT) and in high-temperature environments [11,12]. The MTJ device was deposited on the substrate, which was determined to be compatible with the semiconductor process. However, few researchers have focused on the hardness, Young's modulus, and microstructure of CoFeB thin films. Thus, a study of its mechanical properties, durability, and microstructure is of value. Nano-indentation measurements have yielded extremely useful information on their mechanical properties (hardness and elastic modulus), based on analyses of load–displacement curves [13–16].

This study also investigated the typical CoFeB films to determine their microstructure, magnetic properties and nanomechanical properties by high-resolution transmission electron microscopy (HRTEM), X-ray diffraction (XRD), nano-indentation measurement, and vibrating sample magnetometer (VSM). To determine the grain size distribution and the average grain size, a plane-view microstructure was obtained using HRTEM. The electron diffraction pattern and XRD diffraction peak verified that CoFeB thin films had a body-centered cubic (BCC) structure. Grain refinement increases the magnetic squareness ratio of the CoFeB film, and reduces its coercivity (H_c). The mechanism of grain refinement also increases the hardness and Young's modulus, consistent with the "Hall–Petch" effect.

2. Experimental details

CoFeB thin films were deposited onto a glass substrate by dc magnetron sputtering, with thicknesses (t_f) from 100 to 500 Å under the following three conditions: (a) substrate temperature (T_s) maintained at RT, (b) post-annealing at T_A = 150 °C for 1 h, and (c) post-annealing at T_A = 350 °C for 1 h. The typical base chamber pressure was greater than 1.5×10^{-7} Torr and the Ar working chamber pressure was

* Corresponding author. Tel.: +886 7657 7711; fax: +886 7657 8444.
E-mail address: ytchen@isu.edu.tw (Y.-T. Chen).

0925-8388/$ – see front matter.
doi:10.1016/j.jallcom.2010.03.141

5×10^{-3} Torr. The target composition of the CoFeB alloy was 60 at.% Co, 20 at.% Fe, and 20 at.% B.

The structure of the CoFeB thin film was characterized using XRD with a Cu $K_{\alpha 1}$ line (Philips X'Pert). The plane-view microstructure of the CoFeB thin film was captured using HRTEM (JEOL-2100F). The average grain size distribution was determined by grain size analysis software. The in-plane magnetic hysteresis loop was measured using a LakeShore Model 7300 VSM. The hardness and Young's modulus of the CoFeB thin films were measured using an ultra micro-indentation system (UMIS-2000, CSIRO, Australia) with a Berkovich indenter with a radius of ~50 nm. The UMIS and indenter tips were carefully calibrated using fused silica with known material properties. An indentation load of 1 mN was adopted to limit the depth of penetration of the indenter to less than 10% of the thickness of the film. The indentation load was increased in 40 steps, and the penetration depth was measured at each step. The hardness and Young's modulus were obtained as means of several measurements.

3. Results and discussion

Fig. 1 presents the X-ray diffraction patterns obtained under three conditions. The main peak of the CoFeB-500 Å films in this figure is that of the BCC (110) structure. The broadened peak of CoFeB-500 Å suggests that the as-deposited sample is in a very fine

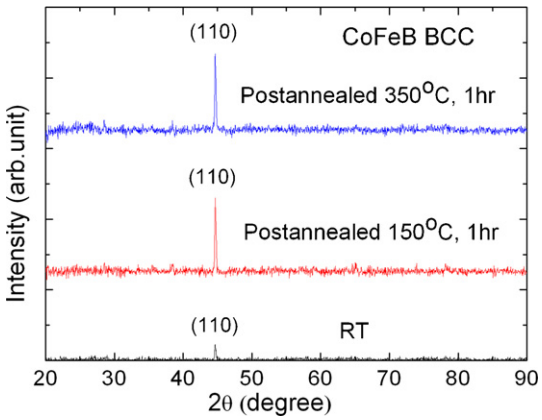

Fig. 1. XRD patterns of BCC 500 Å-thick CoFeB thin films under three conditions.

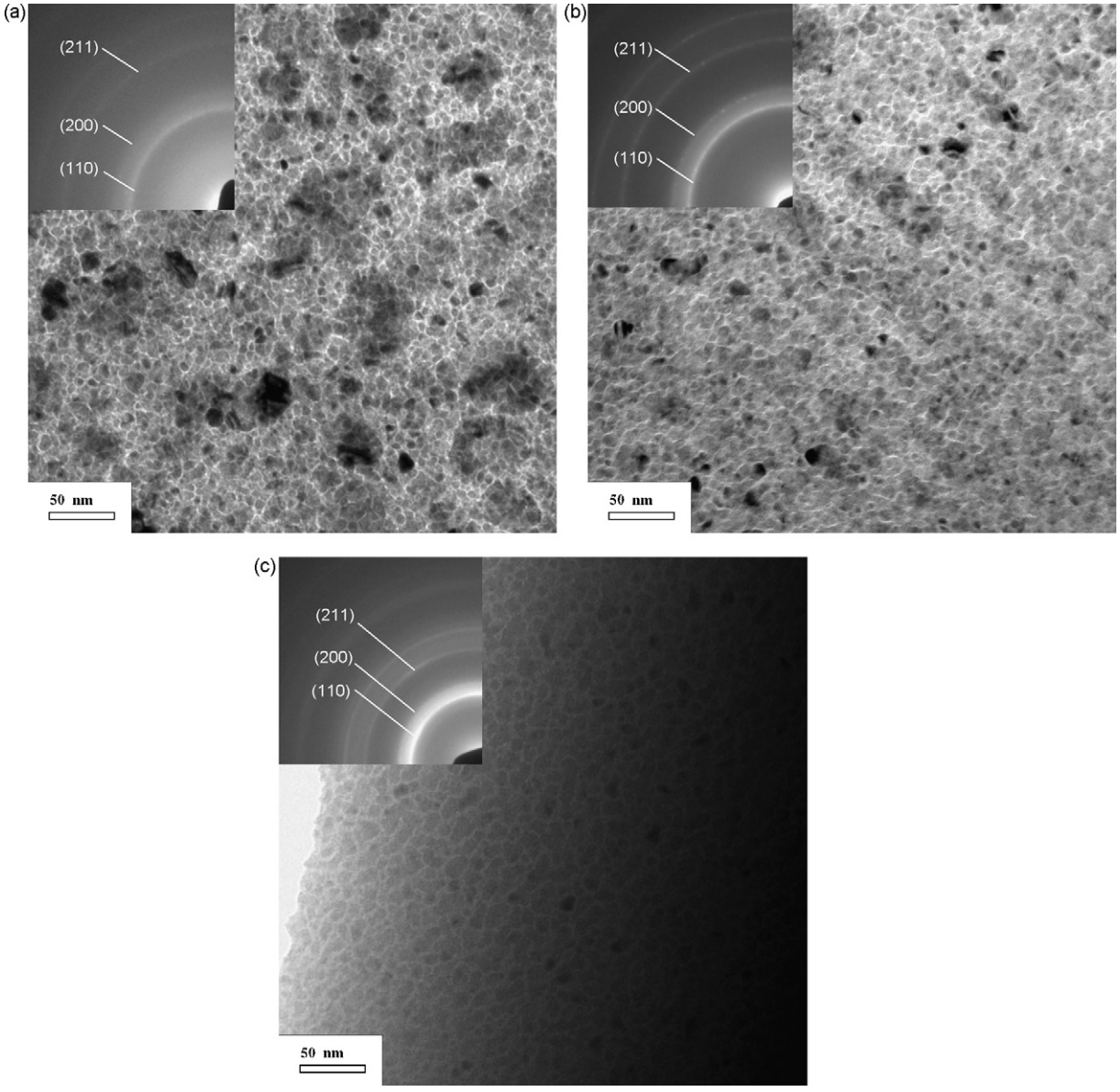

Fig. 2. Plane-view HRTEM images of 500 Å-thick CoFeB thin films under three conditions: (a) deposited at RT only, (b) post-annealed at T_A = 150 °C for 1 h, and (c) post-annealed at T_A = 350 °C for 1 h. The main diffraction patterns in the inset indicate a body-centered cubic (BCC) structure.

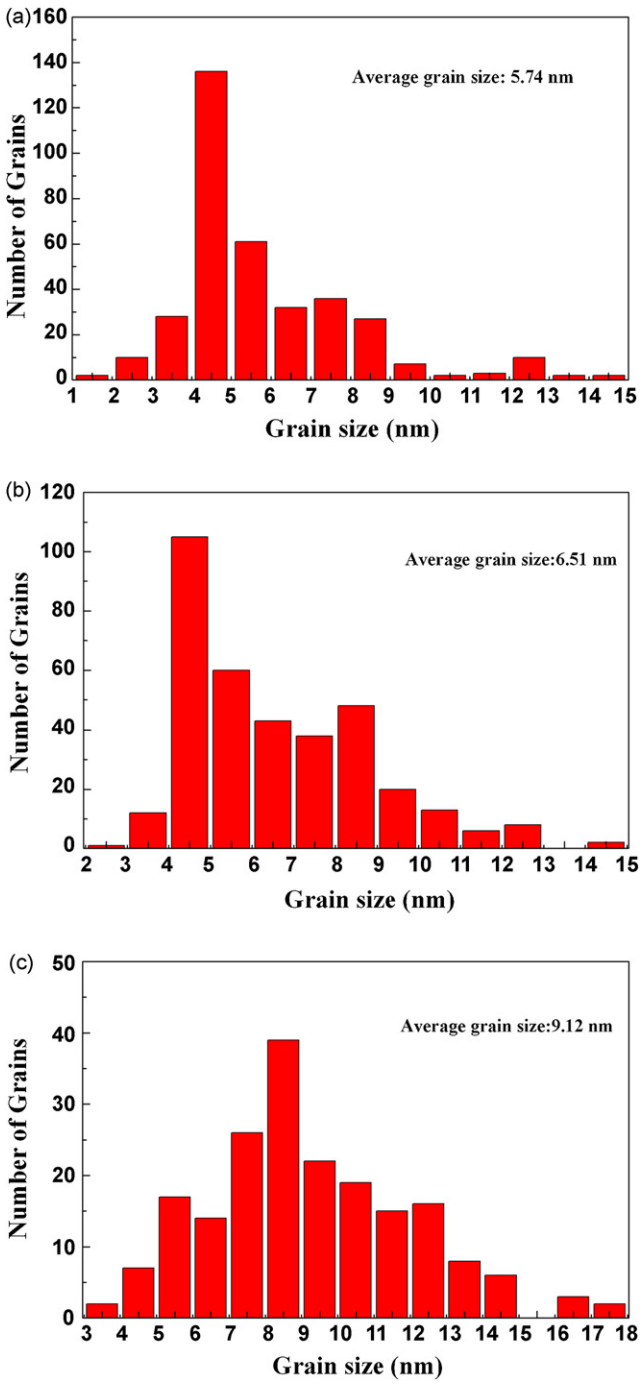

Fig. 3. Histogram presents the grain size distributions in 500 Å-thick CoFeB thin films, (a) deposited at RT only, (b) post-annealed at T_A = 150 °C for 1 h, and (c) post-annealed at T_A = 350 °C for 1 h.

nano-crystalline state at this stage. Furthermore, the post-annealed films are more crystalline than the film at RT, for annealing treatment can provide a driving force for increasing the grain size above that at RT. Scherrer's formula enables the grain size (d) to be estimated from the measured width of the diffraction peak under three different conditions [17]. Scherrer's formula can be described as

$$d = \frac{0.9\lambda}{B\cos\theta}, \quad (1)$$

where λ is the wavelength of the Cu $K_{\alpha 1}$ line, B is the full width half maximum (FWHM) of the (1 1 0) peak, and θ is the half angle of the diffraction peak. Applying Scherrer's formula, the grain sizes

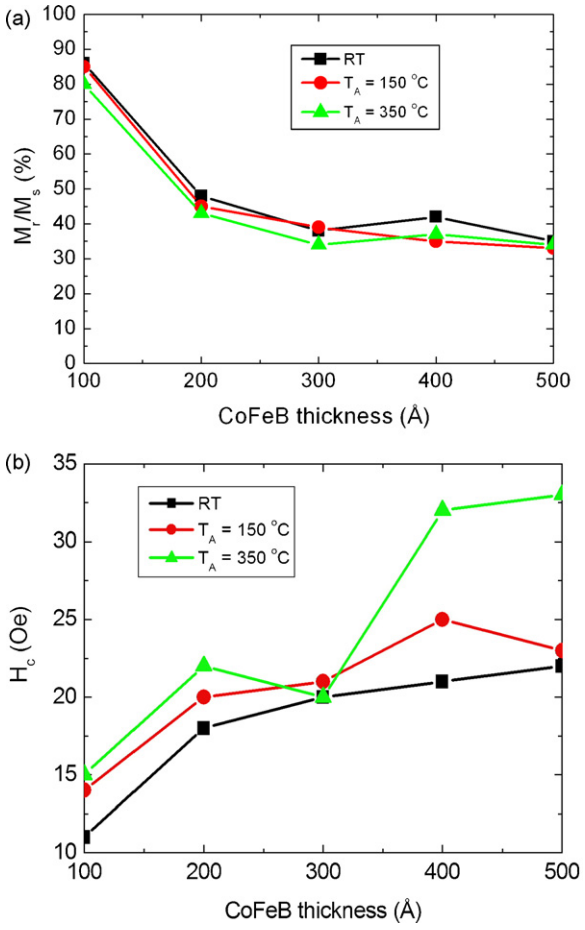

Fig. 4. The magnetic properties of squareness ratio and coercivity of deposited CoFeB film at T_s = RT continuously, and T_s = RT with post-annealing at heat annealing T_A = 150 °C, or 350 °C for 1 h. (a) the squareness (M_r/M_s) ratio and (b) coercivity (H_c).

of CoFeB-500 Å can be determined as such: (a) when the substrate temperature (T_S) is maintained at RT, 62 Å; (b) after post-annealing at T_A = 150 °C for 1 h, 64 Å; and (c) after post-annealing at T_A = 350 °C for 1 h, 71 Å.

Fig. 2(a)–(c) displays the typical plain-view grain size distributions in CoFeB-500 Å films under different conditions, obtained using HRTEM. The grain size distributions are determined from a histogram, which is shown in Fig. 3. The selected-area-diffraction (SAD) pattern in the inset in Fig. 2(a) indicates that the as-deposited CoFeB film is nano-crystalline at RT. The insets in Fig. 2(b) and (c) show grain coarsening as the annealing temperature increases. Since the main diffraction patterns are (1 1 0), (2 0 0), and (2 1 1), the CoFeB films must contain BCC grains. The X-ray diffraction peaks are consistent with the electron diffraction pattern obtained by HRTEM.

Fig. 3 plots the distributions of the grain size, both before and after annealing of the CoFeB films. Fig. 3(a) shows that the as-deposited CoFeB 500 Å-thick film contains grains with sizes following a Gaussian distribution, with an average value of 57 Å. The average grains following annealing at T_A = 150 °C and T_A = 350 °C for 1 h are 65 and 91 Å, as presented in Fig. 3(b) and (c). These results are attributed to the thermally driven dynamic grain coarsening. Fig. 3 demonstrates that grain size increases with temperature.

Fig. 4(a) shows the magnetic squareness (M_r/M_s) ratio of the CoFeB films with the in-plane hysteresis loop, where M_r is the remanent magnetization and M_s is the saturation magnetization, at thicknesses of 100–500 Å under the three conditions of interest. The macroscopic anisotropy of the as-deposited and annealed CoFeB

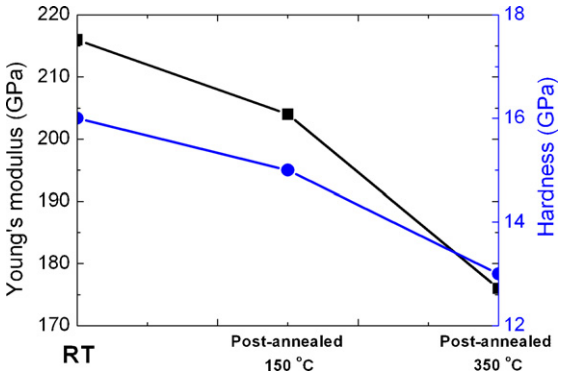

Fig. 5. Hardness and Young's modulus of 500 Å-thick CoFeB thin films under three conditions.

films, detected by in-plane and out-of-plane hysteresis loops, indicates the CoFeB films have in-plane anisotropy. The M_r/M_s ratios of the as-deposited and annealed samples show similar behavior. The refined grain sizes in the as-deposited film show higher M_r/M_s ratio than that following annealing. Previous research suggested that refinement of grains reduces the effective anisotropy constant (K_{eff}) [18]. The relevant formula is

$$L_{\text{ex}} = \pi \left(\frac{A_{\text{eff}}}{K_{\text{eff}}} \right)^{1/2}, \tag{2}$$

where A_{eff} represents the effective exchange stiffness and L_{ex} is the effective exchange range. The reduction in K_{eff} increases the effective exchange range, causing the fine grains to be exchange-coupled, increasing the remanent magnetization and the squareness ratio. Fig. 4(b) reveals that the coercivity (H_c) is dominated by the grain morphology effect under three conditions and indicates that larger grains yield a higher H_c. This result is consistent with the grain size effect [19,20]. About the effect of defect on coercivity, since the as-deposited CoFeB thin films show the nanocrystalline state, it indicates the existence of more grain boundaries at this stage, which leads to decrease effective anisotropy constant (K_{eff}) and coercivity (H_c). In contrast, the existence of few grain boundaries at annealed films, which leads to a strong increase in domain wall pinning and large variation in anisotropy [21,22]. Therefore, the coercivity of annealed CoFeB films is larger than as-deposited samples. As expected, the as-deposited CoFeB films with finer grains have better magnetic properties, such as lower H_c. It indicates the as-deposited CoFeB film is suitable for free layer application of MTJ.

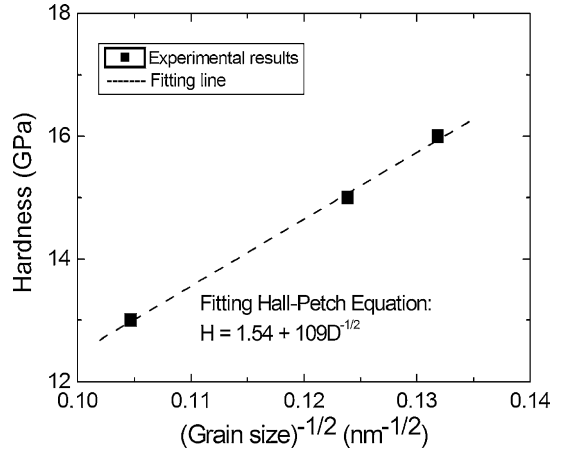

Fig. 6. Experimental hardness as a function of grain size, fitted using Hall–Petch equation.

Fig. 5 plots the results of measurements of Young's modulus (E) and hardness (H) measurement of the CoFeB-500 Å film. Apparently, the nanomechanical values (E, H) decline as the post-annealing temperature increases. The hardness values of the CoFeB thin films that were deposited at T_s = RT and those that underwent post-annealing at T_A = 150 and 350 °C for 1 h were 16, 15, and 13 GPa, respectively. The corresponding Young's moduli were 216, 204, and 176 GPa, respectively. The hardness is well known to depend greatly on grain size, according to the Hall–Petch equation [23]:

$$H = H_i + kD^{-1/2}, \tag{3}$$

where H_i, k and D denote the lattice friction stress, the Hall–Petch constant, and the grain size, respectively. This formula indicates that finer grains are associated with more grain boundaries and thus greater mechanical strength. The dashed line plotted in Fig. 6 was obtained by curve fitting to experimental results based on the Hall–Petch equation:

$$H = 1.54 + 109D^{-1/2}, \tag{4}$$

which specifies a probable lattice friction stress of 1.54 GPa and a Hall–Petch constant of 109 GPa $\text{nm}^{-1/2}$ for CoFeB thin films. The CoFeB film is nanomechanically stronger than the Co film [12]. Since boron (B) atoms were added to the CoFe film, the operation of the refining grain mechanism is reasonable. The hardness and Young's modulus fell as the sizes of the grains in the CoFeB film increased. The grain size histogram distribution obtained from the plain-view TEM image reveals that the post-annealed grains are larger than those occurring at RT. Hence, hardness and Young's modulus are reduced by the enlargement of grains, consistent with the "Hall–Petch" effect [24].

4. Conclusions

The magnetic and nanomechanical characteristics of CoFeB thin films deposited by sputtering under various conditions of RT and post-annealing treatment have been examined. Observations of the grain distribution using plane-view HRTEM, electron diffraction, and XRD show that the CoFeB thin films have a BCC structure. Larger grains are formed by heating than are present at RT. The magnetic properties and nano-indentation analysis indicated that the refining grain mechanism can improve the squareness ratio, coercivity, Young's modulus, and hardness. The nanomechanical result is consistent with the Hall–Petch effect.

Acknowledgements

This work was supported by the National Science Council and I-Shou University, under Grants no. NSC97-2112-M-214-001-MY3 and ISU98-S-02.

References

[1] S. Yuasa, A. Fukushima, H. Kubota, Y. Suzuki, K. Ando, Appl. Phys. Lett. 89 (2006) 042505.
[2] X.F. Han, A.C.C. Yu, J. Appl. Phys. 95 (2004) 764.
[3] M. Sato, K. Kobayashi, Jpn. J. Appl. Phys. 36 (1997) L200.
[4] C. Kim, Y.C. Chung, J. Phys. D 42 (2009) 015003.
[5] Y.T. Chen, S.U. Jen, Y.D. Yao, J.M. Wu, A.C. Sun, Appl. Phys. Lett. 88 (2006) 222509.
[6] S. Yuasa, D.D. Djayaprawira, J. Phys. D 40 (2007) R337.
[7] D.P. Shoemaker, M. Grossman, R. Seshadri, J. Phys. D 20 (2008) 195219.
[8] Y.T. Chen, Nanoscale Res. Lett. 4 (2009) 90.
[9] J. Ni, J.W. Cai, W.Y. Lai, Y.K. An, Z.H. Mai, J. Phys. D 39 (2006) 730.
[10] Y.T. Chen, S.U. Jen, Y.D. Yao, J.M. Wu, J.H. Liao, T.B. Wu, J. Alloys Compd. 448 (2008) 59.
[11] D.M. Jeon, J.W. Park, Y.S. Kim, D.H. Yoon, S.J. Suh, Thin Solid Films 435 (2003) 135.

[12] Y.T. Chen, S.R. Jian, J. Alloys Compd. 481 (2009) 365.
[13] S.U. Jen, Y.T. Chen, N.T. Yang, W.C. Cheng, Appl. Phys. A 94 (2008) 431.
[14] S.R. Jian, Jason S.C. Jang, Y.S. Jang, P.F. Lai, C.S. Yang, H.C. Yang, C.H. Wen, Tsai, Mater. Chem. Phys. 109 (2008) 360.
[15] S.R. Jian, I.J. Teng, P.F. Yang, Y.S. Lai, J.M. Lu, J.G. Chang, S.P. Ju, Nanoscale Res. Lett. 3 (2008) 186.
[16] S.R. Jian, Jason S.C. Jang, G.J. Chen, H.G. Chen, Y.T. Chen, J. Alloys Compd. 479 (2009) 348.
[17] B.D. Cullity, Elements of X-ray Diffraction, 2nd ed., Addison-Wesley, Reading, MA, 1978.
[18] Z.Q. Jin, N.N. Thadhani, M. McGill, J. Li, Z.L. Ding, H. Wang, M. Zeng, S.F. Chen, J.P. Cheng, Liu, J. Appl. Phys. 96 (2004) 3452.
[19] M. Yoshino, Y. Kikuchi, A. Sugiyama, T. Osaka, Electrochim. Acta 53 (2007) 285.
[20] W.S. Sun, T. Kulik, X.B. Liang, J. Ferenc, Intermetallics 14 (2006) 1066.
[21] Y. Sun, R.W. Gao, Solid State Commun. 149 (2009) 393.
[22] J. Zhang, Y.X. Li, F. Wang, B.G. Shen, J.R. Sun, J. Appl. Phys. 107 (2010) 043911.
[23] R. Venkataman, J.C. Bravman, J. Mater. Res. 7 (1992) 2040.
[24] S. Zhang, D. Sun, Y.Q. Fu, H.J. Du, Surf. Coat. Technol. 167 (2003) 113.